2013

On The Cause Of Supra-Arcade Downflows In Solar Flares

P. A. Cassak

J. F. Drake

J. T. Gosling

T.-D. Phan

M. A. Shay

See next page for additional authors

The Astrophysical Journal Letters, 775:L14 (6pp), 2013 September 20 doi:10.1088/2041-8205/775/1/L14

ON THE CAUSE OF SUPRA-ARCADE DOWNFLOWS IN SOLAR FLARES

P. A. Cassak[1], J. F. Drake[2], J. T. Gosling[3], T.-D. Phan[4], M. A. Shay[5], and L. S. Shepherd[1]
[1] Department of Physics and Astronomy, West Virginia University, Morgantown, WV 26506, USA; Paul.Cassak@mail.wvu.edu, lshephe1@mix.wvu.edu
[2] Department of Physics and the Institute for Physical Science and Technology and the Institute for Research in Electronics and Applied Physics, University of Maryland, College Park, MD 20742, USA; drake@umd.edu
[3] Laboratory for Atmospheric and Space Physics, University of Colorado at Boulder, Boulder, CO 80303, USA; Jack.Gosling@lasp.colorado.edu
[4] Space Science Laboratory, University of California, Berkeley, CA 94720, USA; phan@ssl.berkeley.edu
[5] Department of Physics and Astronomy, University of Delaware, Newark, DE 20742, USA; shay@udel.edu
Received 2013 May 3; accepted 2013 August 21; published 2013 September 4

ABSTRACT

A model of supra-arcade downflows (SADs), dark low density regions also known as tadpoles that propagate sunward during solar flares, is presented. It is argued that the regions of low density are flow channels carved by sunward-directed outflow jets from reconnection. The solar corona is stratified, so the flare site is populated by a lower density plasma than that in the underlying arcade. As the jets penetrate the arcade, they carve out regions of depleted plasma density which appear as SADs. The present interpretation differs from previous models in that reconnection is localized in space but not in time. Reconnection is continuous in time to explain why SADs are not filled in from behind as they would if they were caused by isolated descending flux tubes or the wakes behind them due to temporally bursty reconnection. Reconnection is localized in space because outflow jets in standard two-dimensional reconnection models expand in the normal (inflow) direction with distance from the reconnection site, which would not produce thin SADs as seen in observations. On the contrary, outflow jets in spatially localized three-dimensional reconnection with an out-of-plane (guide) magnetic field expand primarily in the out-of-plane direction and remain collimated in the normal direction, which is consistent with observed SADs being thin. Two-dimensional proof-of-principle simulations of reconnection with an out-of-plane (guide) magnetic field confirm the creation of SAD-like depletion regions and the necessity of density stratification. Three-dimensional simulations confirm that localized reconnection remains collimated.

Key words: magnetic fields – magnetic reconnection – Sun: activity – Sun: atmosphere – Sun: corona – Sun: flares

1. INTRODUCTION

Supra-arcade downflows (SADs) are dark features at the tops of coronal arcades that descend sunward during solar flares (McKenzie & Hudson 1999; McKenzie 2000). They are important because they provide a window into the spatiotemporal evolution of the magnetic reconnection process that releases energy by changing magnetic topology during solar flares. For example, the standard model of solar flares (e.g., Carmichael 1964; Sturrock 1966; Hirayama 1974; Kopp & Pneuman 1976) depicts a single monolithic reconnection site, but the burstiness and patchiness of SADs suggests that reconnection is patchy and bursty as well. This suggests that reconnection occurs at multiple sites in an extended region rather than along a single line.

There have been many observational studies of SADs, also called "tadpoles" because of their sinuous shape. Their darkness is due to a lack of emitting particles: they persist in soft X-ray and EUV, corresponding to temperatures of 10^4–10^7 K (Innes et al. 2003). Their sunward speed is 45–500 km s^{-1}, below typical coronal Alfvén speeds of 1000 km s^{-1} (McKenzie 2000), though they can be considerably faster (Liu et al. 2013). They decelerate at $\sim$1500 m s^{-2} and last a few minutes (Sheeley et al. 2004). They are correlated with bursts of hard X-rays, suggesting an association with reconnection at the flare site (Asai et al. 2004). They are most easily seen in the decay phase of long duration events (McKenzie 2000), but they begin during the rise phase and persist during hard X-ray bursts (Khan et al. 2007).

Statistical studies of SADs revealed their cross-sectional areas are a few to 70 times 10^6 km^2 (a radius of 1–4 Mm), their mean flux is $\sim 10^{18}$ Mx, they release 10^{27}–10^{28} erg of energy, and their densities are 5–43 times lower than ambient densities (McKenzie & Savage 2009; Savage & McKenzie 2011). They originate at heights of 100–200 Mm and penetrate 20–50 Mm (Savage et al. 2010; Savage & McKenzie 2011). Their areas have a log-normal distribution, and their fluxes are consistent with both log-normal and exponential distributions (McKenzie 2011). Reconnection inflows and outflows near SADs were recently observed (Savage et al. 2012a).

The explanation of their cause remains under debate. They were originally thought of as flux tubes contracting under tension after reconnection (McKenzie & Hudson 1999; McKenzie 2000). Asai et al. (2004) support their relation to reconnection outflows. From the side, the whole loop should be visible; these SAD loops were observed (Savage et al. 2010; Warren et al. 2011). Recently, it was argued that SADs are not flux tubes themselves, but wakes behind them (Savage et al. 2012b). It has also been suggested that they are caused by upflowing matter (Verwichte et al. 2005).

There have only been a few simulation studies of SADs. Seminal studies of flux tubes produced by short-lived patchy three-dimensional (3D) reconnection (Linton & Longcope 2006; Longcope et al. 2010) in the vein of Semenov et al. (1983) reproduced some aspects of SADs, including a teardrop-shaped cross section (Linton & Longcope 2006), deceleration as they reach underlying arcades (Linton et al. 2009), and trailing density voids (Guidoni & Longcope 2011). The evolution of retracting flux tubes were also studied (Shimizu et al. 2009). It was suggested that SADs are generated by interfering shocks ahead of locations where energy is deposited by reconnection (Costa et al. 2009; Schulz et al. 2010; Maglione et al. 2011; Cécere et al. 2012).

In an avenue of research that may be relevant to SAD statistics, a Vlasov-type equation for plasmoids predicts an exponential distribution of sizes (Fermo et al. 2010, 2011; Uzdensky et al. 2010; Huang & Bhattacharjee 2012). The distribution of plasmoid sizes in resistive magnetohydrodynamics was exponential, consistent with observations if corrected for resolution constraints in detecting small SADs (Guo et al. 2013).

There are significant unresolved theoretical issues about present interpretations of SADs. For example, if SADs are either flux tubes or wakes behind them, why does the ambient coronal plasma not rapidly "fill in" the region behind them? If SADs are caused by patchy reconnection, what causes reconnection to start and stop so rapidly?

We argue that SADs are caused by downflowing outflow jets from reconnection that is localized in space but not time, as opposed to isolated flux tubes. New elements of the present model are (1) the importance of density stratification of the solar corona and (2) the role of continuous reconnection as opposed to bursty reconnection in preventing the corona from filling in the region behind SADs. We perform proof-of-principle two-dimensional (2D) simulations that verify this mechanism produces SAD-like density depletions and show the necessity of density stratification. We show in 3D simulations that localized reconnection is necessary to keep the outflow jets collimated. The model is described in Section 2. The simulations are described in Section 3, results are in Section 4, and a discussion is in Section 5.

2. A MODEL OF SADs

Consider a coronal arcade with an overlying vertical current sheet, sketched in Figure 1(a). When reconnection begins at the current sheet, sunward and anti-sunward outflow jets are formed; the sunward jet is shown by the vertical (blue) arrow. Being relatively high in the corona, the plasma at the reconnection site has a relatively low density because the corona is stratified. The relatively higher density plasma in the underlying arcade is denoted by the shaded region. Since the density scale height for coronal parameters is $H \simeq 30$–60 Mm, a jet penetrating tens of Mm sees a significant density change. The density contrast can become larger as chromospheric evaporation populates the arcade. The low density plasma penetrates the denser material below, forming a thin region of lower density plasma. We argue this density depletion is a SAD.

This model raises a question about the shape of SADs. In standard models of 2D steady-state fast reconnection, the outflow jet expands outward in the normal direction in Petschek-type exhausts (Petschek 1964). A similar expansion for bursty reconnection was described as a snow plow effect (Semenov et al. 1998) caused by the retracting flux tube surrounding increasingly more mass. Due to the large length scales between the reconnection site and the looptop, one might expect the broadened jet to create a depletion region wider than seen in observations. However, it was argued that the snow plow effect does not occur in 3D localized reconnection if there is an out-of-plane (guide) magnetic field because the reconnection expands along the guide field instead of the inflow direction, which accommodates the mass that causes expansion in 2D (Linton & Longcope 2006). The guide field during flares has been estimated to be comparable to the reconnecting magnetic field (Qiu 2009; Qiu et al. 2010; Shepherd & Cassak 2012), so this limit is relevant for solar flares.

Since the region of the corona in question has a low plasma β (the ratio of gas pressure to magnetic pressure), the mass is not

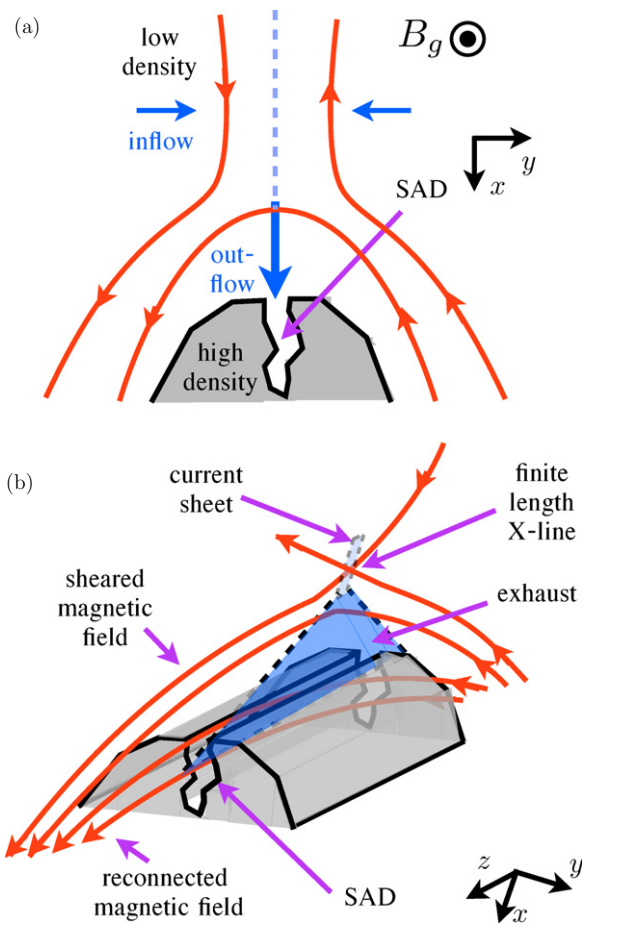

Figure 1. (a) Schematic diagram of the model of SADs. Red lines are magnetic fields. The vertical dashed blue line is the reconnection site high in the corona with a lower density plasma. The blue arrows are the reconnection inflow and sunward outflow. The SAD is caused by the low density outflow impinging on the high density arcade (in gray). (b) Perspective view showing sheared magnetic fields with a finite length X-line and reconnected fields threading the SAD formed by the exhaust.

expected to control the magnetic structure of the reconnection exhaust, so we motivate the result of Linton & Longcope (2006) solely in terms of conservation of magnetic flux. Consider a recently reconnected flux tube with flux $\Delta\Phi$ formed by reconnection at an X-line of finite extent l_z in the out-of-plane direction z and length Δl_x in the outflow direction x. Just downstream of the X-line,

$$\Delta\Phi \sim B_y l_z \Delta l_x, \tag{1}$$

where B_y is the reconnected (normal) component of the magnetic field. After the flux tube has convected downstream, the magnetic field in the exhaust is predominantly in the z direction, so the flux is

$$\Delta\Phi' = B l_y' \Delta l_x, \tag{2}$$

where l_y is the width of the flux tube in the y direction, $B = |\mathbf{B}|$ is the magnitude of the total magnetic field, and the prime denotes post-convection downstream. By conservation of flux, $\Delta\Phi = \Delta\Phi'$, so solving Equations (1) and (2) for l_y' gives

$$l_y' \sim l_z \frac{B_y}{B}. \tag{3}$$

Regardless of whether reconnection is 2D or 3D, the maximum value of B_y is approximately 0.1 of the reconnecting magnetic

field B_x since the normalized rate of fast reconnection is close to 0.1. Equation (3) shows that the maximum downstream expansion of the exhaust l'_y is proportional to l_z. In quasi-2D systems, l_z is large and the exhaust gets wider with downstream distance. In 3D localized reconnection, l'_y has an upper limit, so the exhaust is collimated. For the present application, this implies the density depletion regions formed by finite length X-lines are thin, consistent with observations of SADs.

A sketch with a perspective 3D view is shown in Figure 1(b), illustrating the difference between the present model and models with SADs as isolated flux tubes or wakes behind them (Savage et al. 2012b). In the flux tube model, reconnection happens for a short time, leading to a single flux tube propagating sunward. In the present model, the reconnection is continuous in time, at least long enough for the material ejected sunward to propagate to the looptop. Therefore, reconnected magnetic field threads the entire extent of the depletion region, not just through a single flux tube. This explains why plasma does not rapidly fill in behind the SAD as would occur if it were an isolated flux tube. Further comparison to previous work is presented in Section 5.

3. SIMULATIONS

Simulations are performed using the two-fluid code F3D (Shay et al. 2004). Magnetic fields and number densities are normalized to arbitrary values B_0 and n_0. Lengths are normalized to the ion inertial scale $d_{i,0} = c/\omega_{pi,0}$, the scale where the Hall effect is important, where $\omega_{pi,0} = (4\pi n_0 e^2/m_i)^{1/2}$ is the plasma frequency, and e and m_i are the ion charge and mass. Times are normalized to the inverse ion cyclotron frequency Ω_{ci}^{-1}, velocities to the Alfvén speed, and pressures to $B_0^2/4\pi$. All simulations have periodic boundary conditions in each direction.

The 2D simulations have 2048×512 cells in a system of size $L_x \times L_y = 102.4 \times 25.6$. The continuity, momentum, ion pressure, and induction equations are evolved in time. The electric field is given by the generalized Ohm's law (in cgs units)

$$\mathbf{E} = -\frac{\mathbf{v}_i \times \mathbf{B}}{c} + \frac{\mathbf{J} \times \mathbf{B}}{nec} + \frac{m_e}{e^2}\frac{d(\mathbf{J}/n)}{dt}, \quad (4)$$

where $\mathbf{E}$, $\mathbf{v}_i$, $\mathbf{B}$, and $\mathbf{J}$ are the electric field, ion bulk flow velocity, magnetic field, and current density, respectively, n is the number density and c is the speed of light. Electron inertia m_e is included with $m_e = m_i/25$; this value has been used often and does not affect the reconnection rate (e.g., Shay & Drake 1998). Ions are assumed to be adiabatic with a ratio of specific heats $\gamma = 5/3$ and electrons are assumed to be cold.

The equilibrium consists of a double Harris sheet for the reconnecting magnetic field B_x:

$$B_x(y) = 1 + \tanh\left(\frac{y - y_0}{w_0}\right) - \tanh\left(\frac{y + y_0}{w_0}\right) \quad (5)$$

with an initial current sheet thickness $w_0 = 1$ and field reversal locations of $\pm y_0 = \pm L_y/4$. The equilibrium density profile $n(y)$ is

$$n(y) = 1 + (n_p - 1)\left[\mathrm{sech}^2\left(\frac{y - y_0}{w_0}\right) + \mathrm{sech}^2\left(\frac{y + y_0}{w_0}\right)\right], \quad (6)$$

which is 1 far from the current sheets and n_p at $y = \pm y_0$. The temperature is initially uniform at $T = 1$. To balance total pressure, a guide field B_z is employed with $B_z = 3$ asymptotically far from the current sheets and a profile that balances total pressure. Reconnection is initiated by a magnetic perturbation $\delta\mathbf{B} = -(0.012 B_0 L_y/2\pi)\hat{\mathbf{z}} \times \nabla(\sin(2\pi x/L_x)\sin^2(2\pi y/L_y))$, and a very small incoherent magnetic perturbation is used to break symmetry.

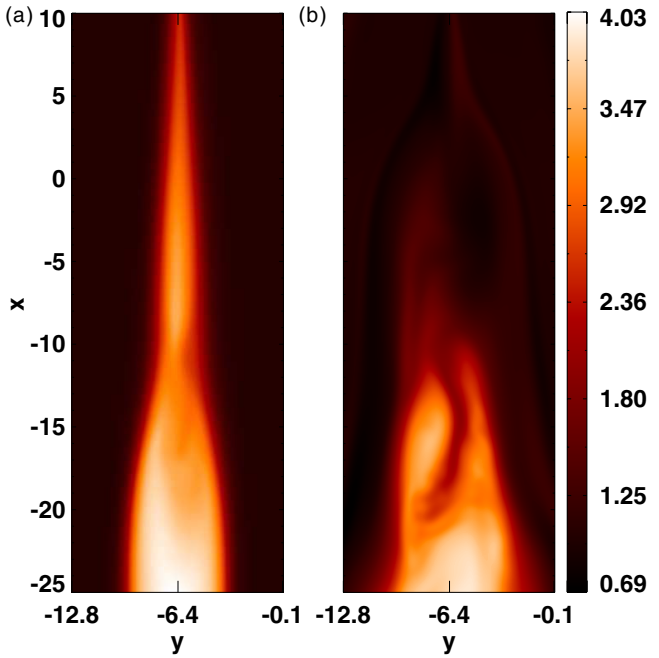

Figure 2. Plasma density for the $n_p = 4$ simulation at (a) $t = 150$ and (b) $t = 210$. The presence of a density depletion is clear in (b).

The 3D simulations have a system size of $51.2 \times 25.6 \times 256$ with $1024 \times 512 \times 256$ grid cells. The equilibrium is the same as in 2D with $n_p = 1.5$ and $w_0 = 0.2$. For this choice of n_p, a uniform guide field $B_z = 3$ enforces pressure balance. The ions are isothermal in the 3D simulations.

Since reconnection with a guide field and the Hall and electron inertia terms in Equation (4) naturally spreads in the out-of-plane direction (Shepherd & Cassak 2012), we omit these terms but include a localized (anomalous) resistivity η_{anom} to achieve fast reconnection of finite extent. The form of η_{anom} is

$$\eta_{\mathrm{anom}} = \eta_0 e^{-(x^2+y^2)/w^2}\frac{(\tanh(z + w_z) - \tanh(z - w_z))}{2}, \quad (7)$$

where $\eta_0 = 0.01$, $w = 0.5$, and w_z is a parameter controlling the half-length of the reconnection X-line in the out-of-plane direction.

This equilibrium should be treated solely as a numerical device to set up a stratified plasma in the outflow direction. The initial conditions are stratified in the inflow direction, but when reconnection begins, it processes this material and populates the arcade with the high density plasma. When the lower density material convects to the reconnection site, the outflow jet is ejected into a vertically stratified arcade as desired.

4. RESULTS

First, we show that SAD-like depletions occur using $n_p = 4$ for the peak density. As time evolves, the high density plasma initially at the current sheet is corralled into the arcade by reconnection early in the simulation (Figure 2(a) at $t = 150$). When the lower density plasma reaches the reconnection site, it populates the outflow jet and penetrates the high density arcade (Figure 2(b) at $t = 210$). A sinuous plasma depletion is clearly

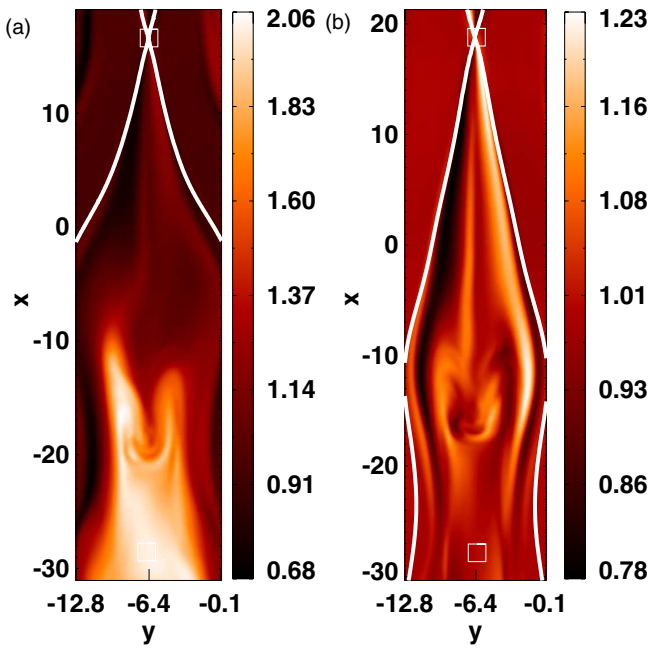

Figure 3. Plasma density for simulations with initial peak density n_p of (a) 2 and (b) 1, showing that SAD-like depletions require density stratification to occur.

seen. Therefore, reconnection can carve a density depletion into a higher density arcade.

To test the importance of density stratification, simulations with different n_p are performed. Figure 3(a) shows the density in a simulation with $n_p = 2$ instead of 4. The white line marks the separatrix (the outermost closed field line), and the white boxes at the top and bottom denote the X- and O-line, respectively. A SAD-like depletion is clearly present. Panel (b) has an initially uniform density ($n_p = 1$). While a curved structure does appear, it is not a depletion as for $n_p > 1$. Therefore, the simulations suggest that density stratification is a key ingredient of SAD-like depletions.

Based on the results of Figure 2, one might conclude that a 2D model with density stratification is sufficient to explain SADs. However, we argue there are two reasons the density depletion cannot propagate the large distances required to explain SADs in 2D. First, as discussed in Section 2, fast reconnection in 2D has an exhaust that expands as in the Petschek model, which is inconsistent with the collimated structure of SADs. Second, the depletion region in Figure 2(b) stretches the reconnected field so that the field wraps around the front of the jet, producing a backward tension force that slows the jet. In 3D reconnection with a finite length X-line, both of these problems are fixed.

To see that outflow jets in 2D fast reconnection broaden with distance from the X-line while localized 3D reconnection leads to collimated exhausts as seen in the observations, we present 3D simulations with $n_p = 1.5$. The reconnection outflow v_x is shown in Figures 4(a) through (c) for $w_z = 60$, 30, and 10, respectively. The vertical lines are a distance 0.5 from the neutral line. The jet broadens continuously for the longest X-line simulation in panel (a), which for the present computational domain is essentially a 2D case. (Note that this is true because of the finite size of the computational domain; 3D effects would be seen if the system was larger in the x direction.) The width of the exhaust remains limited when reconnection is more localized in the z direction as in panel (c). A 3D visualization of the exhaust jets and threading of the magnetic fields for the $w_z = 10$ simulation is given in Figure 5(a), which shows that the exhaust is localized in the y direction and expands in the z direction. Unlike in the 2D simulations, the reconnected field lines in red threading the exhaust are straight (which is obscured in the figure but can be seen when the exhaust isosurface in blue is removed), which implies there is no backward tension force slowing the exhaust in 3D. Panel (b) shows the same data with the exhaust removed and rotated to more clearly see the 3D density depletion in the underlying arcade. Thus, 3D

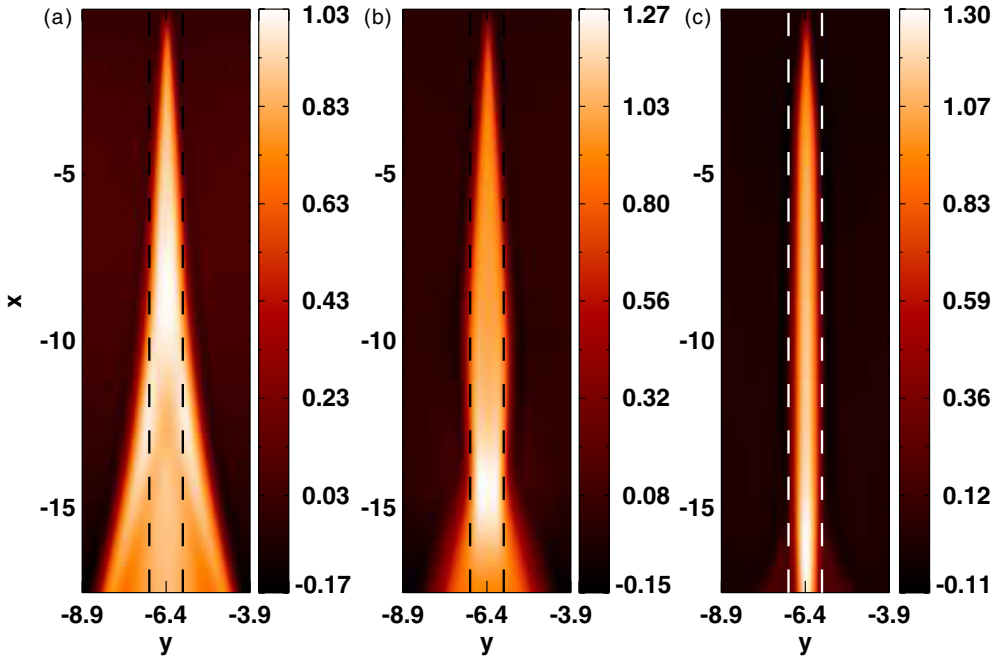

Figure 4. Results for 3D simulations with anomalous resistivity localized in the out-of-plane direction. The outflow v_x is shown for $w_z =$ (a) 60, (b) 30, and (c) 10, revealing that the jet becomes increasingly collimated for reconnection sites that are more localized in the out-of-plane direction.

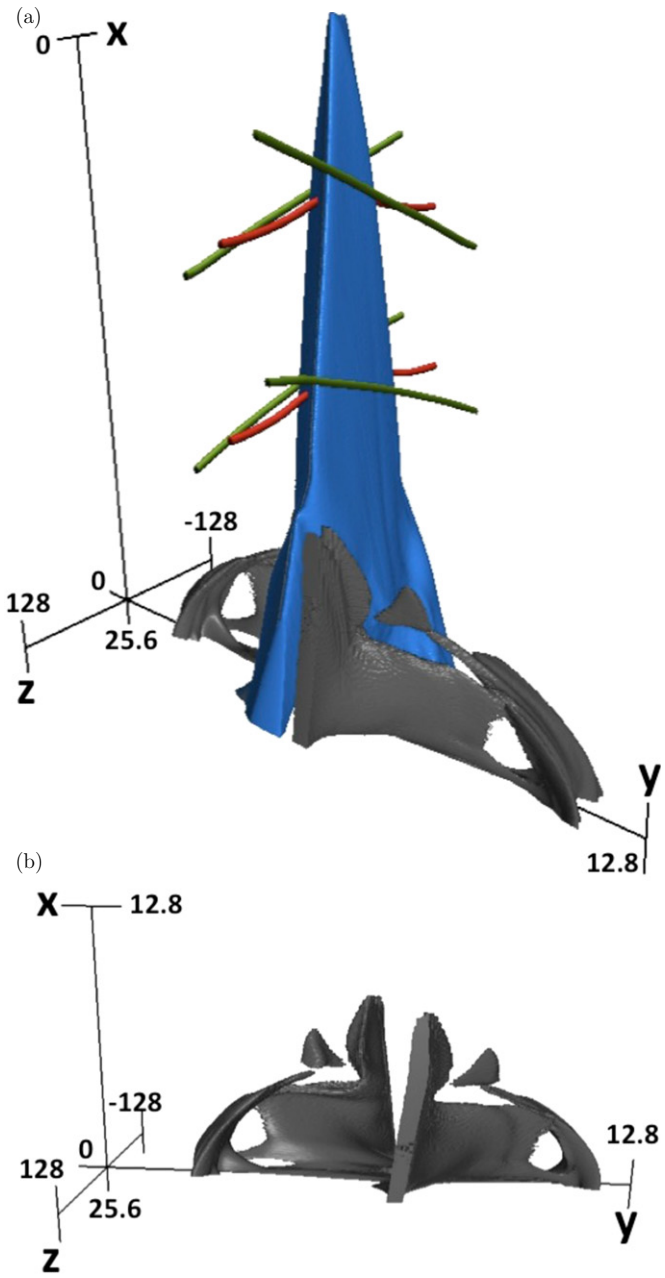

Figure 5. (a) 3D view from the $w_z = 10$ simulation of isosurfaces of the outflow speed (in blue) showing the exhaust spreading in z but not y and a relatively high value of density (gray) showing the depletion carved into the arcade. Representative unreconnected (red) and reconnected (green) magnetic field lines are shown. (b) The density isosurface from panel (a) rotated to reveal the 3D SAD-like density depletion.

spatial localization of reconnection causes exhaust collimation, a necessary ingredient to explain SADs.

5. DISCUSSION

We have presented a model with the critical physics for SAD formation being (1) density stratification of the corona so that the outflow jet can carve out a depletion, (2) reconnection being continuous instead of bursty to prevent the coronal plasma from filling in behind the SAD, and (3) localization of the reconnection site in the out-of-plane direction in order for the outflow jet to remain collimated over the large distances. Proof-of-principle simulations confirm these three basic features.

The present model differs from previous ones in a number of important ways and has a number of appealing aspects because it potentially answers open questions about SADs. Previous models suggested SADs are a result of spatially localized and temporally bursty reconnection. It is not clear why reconnection stops abruptly. In the present model, SADs are localized in space but not in time. We argue the observed burstiness of SADs arises from the abrupt onset of reconnection in disparate spatially localized regions.

A very important question about the interpretation of SADs as flux tubes or wakes behind them is why the high density corona does not rapidly fill in behind the descending flux tube. If it did, SADs would appear as a descending circle instead of an extended depletion. In our model, elongated depletions are a natural consequence of their formation as collimated reconnection outflow jets. An alternative explanation within the flux tube model has been explored in terms of peristaltic flow (Scott et al. 2013).

Asai et al. (2004) previously discussed the correlation of SADs with reconnection outflows, but no clear distinction was made between outflow jets and plasmoids ejected from the reconnection site. There are outward similarities between the present model and one by Costa et al. (2009), Schulz et al. (2010), Maglione et al. (2011), and Cécere et al. (2012). These studies used a pressure pulse to emulate the effect of energy deposition from reconnection. It was argued that shocks and waves generated from the pulse interfere to produce voids. This occurs even in a uniform plasma, while here the reconnection jet itself carves the SAD and requires density stratification. With the exception of Cécere et al. (2012), we know of no previous simulation study to include density stratification.

The present model has similarities to a leading model for low density plasma bubbles propagating earthward in the Earth's magnetotail (Pontius & Wolf 1990), though there are some differences. In both models, reconnection jets impinge on a higher density region underlying the reconnection site. In the magnetotail, an extended reconnection X-line in the out-of-plane direction forms and breaks up due to interchange into numerous flow channels (Wiltberger et al. 2000). Here, we argue the X-line is spatially localized, leading to a single flow channel.

Of course, SAD-like depletions in simulations should not be overstated as real SADs. The many similarities to observed SADs are qualitative rather than quantitative. Future work will require quantitatively investigating whether the following properties in the simulations agree with observations: sub-Alfvénic sunward speed, deceleration, duration, penetration depth, sizes, and energy content.

The authors gratefully acknowledge support from NSF grants AGS-0953463 (P.A.C.), AGS-1202330 (J.F.D.), ATM-0645271 (M.A.S.) and NASA grants NNX10AN08A (P.A.C.), NNX10AC01G (J.T.G.), NNX08AO83G (T.D.P.), and NNX08AO84G (J.T.G.) and acknowledge beneficial conversations with J. T. Karpen, W. Liu, J. C. Raymond, and M. I. Sitnov. This research used resources of the National Energy Research Scientific Computing Center.

REFERENCES

Asai, A., Shibata, K., Yokoyama, T., & Shimogo, M. 2004, in ASP Conf. Ser. 325, Solar-B Mission and the Forefront of Solar Physics, ed. T. Sakurai & T. Sekii (San Francisco, CA: ASP), 361

Carmichael, H. 1964, in AAS/NASA Symposium on the Physics of Solar Flares, ed. W. N. Ness (Washington, DC: NASA), 451

Cécere, M., Schneiter, M., Costa, A., Elaskar, S., & Maglione, S. 2012, ApJ, 759, 79
Costa, A., Elaskar, S., Fernandez, C. A., & Martinez, G. 2009, MNRAS, 400, L85
Fermo, R. L., Drake, J. F., & Swisdak, M. 2010, PhPl, 17, 010702
Fermo, R. L., Drake, J. F., Swisdak, M., & Hwang, K. J. 2011, JGR, 116, A09226
Guidoni, S. E., & Longcope, D. W. 2011, ApJ, 730, 90
Guo, L. J., Bhattacharjee, A., & Huang, Y.-M. 2013, ApJL, 771, L14
Hirayama, T. 1974, SoPh, 34, 323
Huang, Y.-M., & Bhattacharjee, A. 2012, PhRvL, 109, 265002
Innes, D. E., McKenzie, D. E., & Wang, T. 2003, SoPh, 217, 247
Khan, J. I., Bain, H. M., & Fletcher, L. 2007, A&A, 475, 333
Kopp, R. A., & Pneuman, G. W. 1976, SoPh, 50, 85
Linton, M. G., DeVore, C. R., & Longcope, D. W. 2009, EP&S, 61, 573
Linton, M. G., & Longcope, D. W. 2006, ApJ, 642, 1177
Liu, W., Chen, Q. R., & Petrosian, V. 2013, ApJ, 767, 168
Longcope, D. W., Jardins, A. C. D., Carranza-Fulmer, T., & Qiu, J. 2010, SoPh, 267, 107
Maglione, L. S., Schneiter, E. M., Costa, A., & Elaskar, S. 2011, A&A, 527, L5
McKenzie, D. E. 2000, SoPh, 195, 381
McKenzie, D. E. 2011, ApJL, 735, L6
McKenzie, D. E., & Hudson, H. S. 1999, ApJL, 519, L93
McKenzie, D. E., & Savage, S. L. 2009, ApJ, 697, 1569
Petschek, H. E. 1964, in AAS/NASA Symposium on the Physics of Solar Flares, ed. W. N. Ness (Washington, DC: NASA), 425
Pontius, D. H., Jr., & Wolf, R. A. 1990, GeoRL, 17, 49
Qiu, J. 2009, ApJ, 692, 1110
Qiu, J., Liu, W., Hill, N., & Kazachenko, M. 2010, ApJ, 725, 319
Savage, S. L., Holman, G., Reeves, K. K., et al. 2012a, ApJ, 754, 13
Savage, S. L., & McKenzie, D. E. 2011, ApJ, 730, 98
Savage, S. L., McKenzie, D. E., & Reeves, K. K. 2012b, ApJL, 747, L40
Savage, S. L., McKenzie, D. E., Reeves, K. K., Forbes, T. G., & Longcope, D. W. 2010, ApJ, 722, 329
Schulz, W., Costa, A., Elaskar, S., & Cid, G. 2010, MNRAS, 407, L89
Scott, R. B., Longcope, D. W., & McKenzie, D. E. 2013, ApJ, in press
Semenov, V. S., Heyn, M. F., & Kubyshkin, I. V. 1983, SvA, 27, 660
Semenov, V. S., Volkonskaya, N. N., & Biernat, H. K. 1998, PhPl, 5, 3242
Shay, M. A., & Drake, J. F. 1998, GeoRL, 25, 3759
Shay, M. A., Drake, J. F., Swisdak, M., & Rogers, B. N. 2004, PhPl, 11, 2199
Sheeley, N. R., Jr., Warren, H. P., & Wang, Y.-M. 2004, ApJ, 616, 1224
Shepherd, L. S., & Cassak, P. A. 2012, JGR, 117, A10101
Shimizu, T., Kondo, K., Ugai, M., & Shibata, K. 2009, ApJ, 707, 420
Sturrock, P. A. 1966, Natur, 211, 695
Uzdensky, D. A., Loureiro, N. F., & Schkochihin, A. A. 2010, PhRvL, 105, 235002
Verwichte, E., Nakariakov, V. M., & Cooper, F. C. 2005, A&A, 430, L65
Warren, H. P., O'Brien, C. M., & Sheeley, N. R., Jr. 2011, ApJ, 742, 92
Wiltberger, M., Pulkkinen, T. I., Lyon, J. G., & Goodrich, C. C. 2000, JGR, 105, 27649